Analyst

Accepted Manuscript

ROYAL SOCIETY OF CHEMISTRY

www.rsc.org/analyst

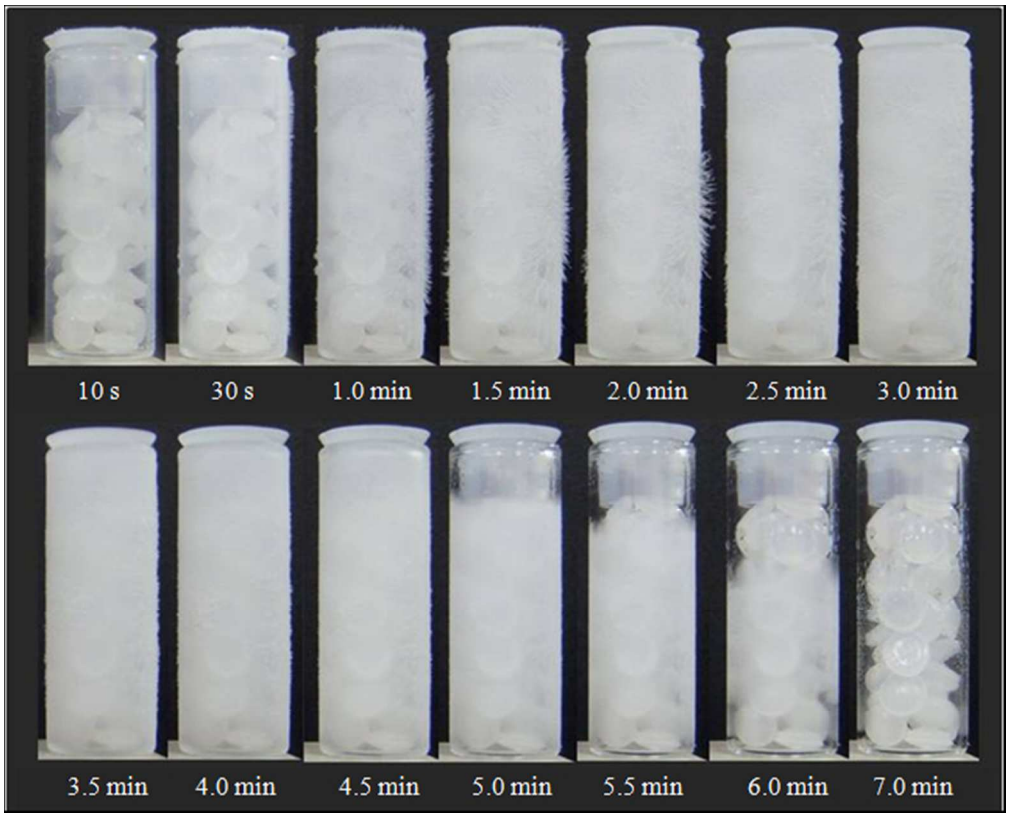

Pictures of the low density PE pellets (density: 0.918 g•cm-3) in a glass vial during the temperature elevation from cryogenic to near room temperature.
108x87mm (150 x 150 DPI)

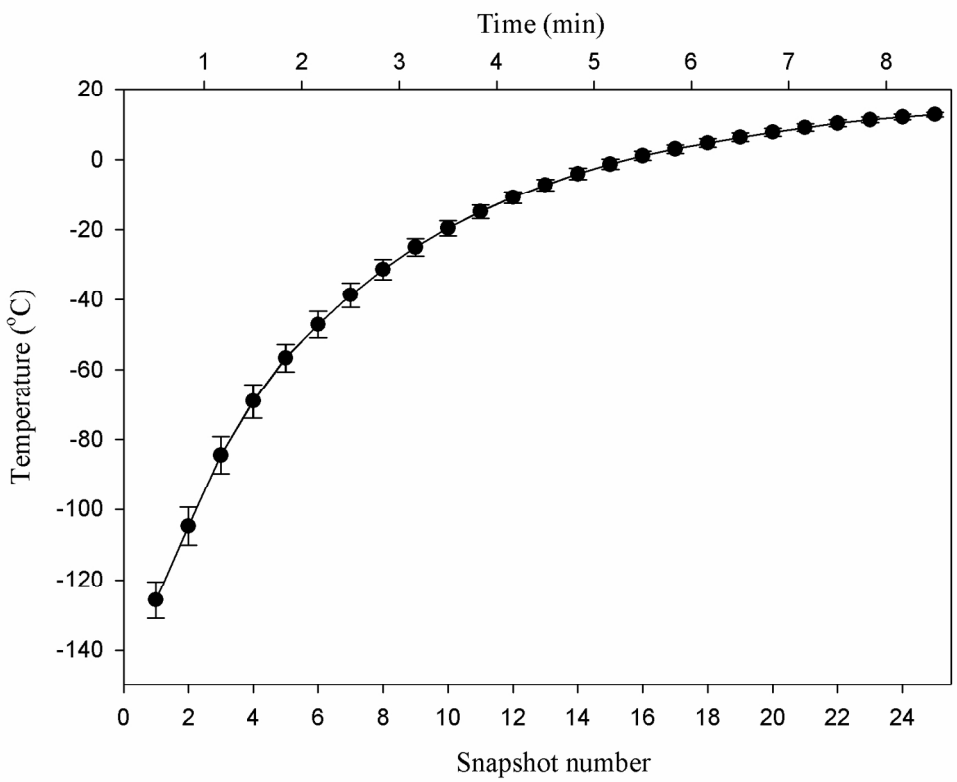

Temperature variation of PE pellets as a function of time, in which the x-axis is designated by both time and snapshot number. The curve corresponds to the average of five independent temperature measurements from five separate batches prepared from the same PE pellets. Bars in each snapshot indicate the corresponding standard deviations of temperature measurements
150x118mm (300 x 300 DPI)

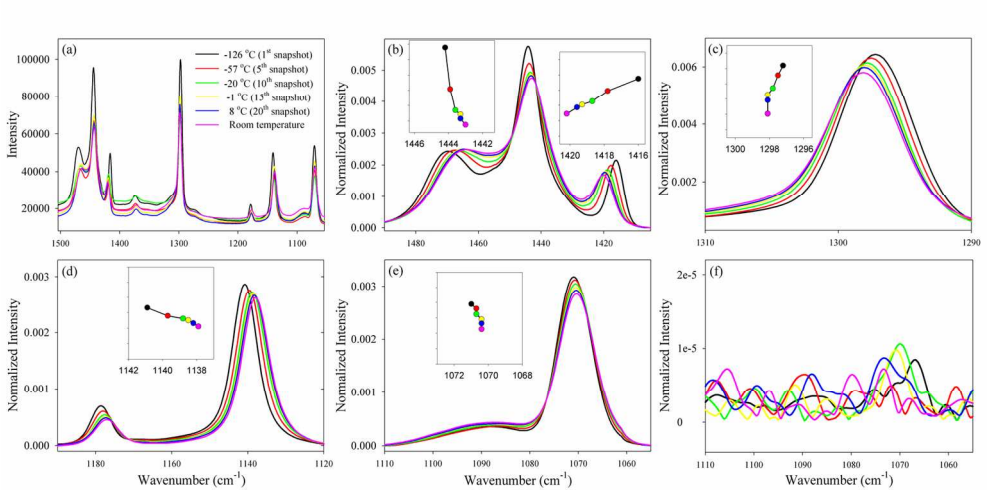

(a) Raman spectra of the PE sample (density: 0.918 g•cm-3) collected during different snapshots in the 1504-1054 cm-1 range. To examine the spectral features in detail, the corresponding normalized spectra were highlighted in four different narrower spectral ranges: (b) 1490-1405, (c) 1310-1290, (d) 1190-1120 and (e) 1110-1055 cm-1. Standard deviations (SDs) of intensities in the 1110-1055 cm-1 range calculated using independently collected triplicate spectra are also shown (f).
154x75mm (300 x 300 DPI)

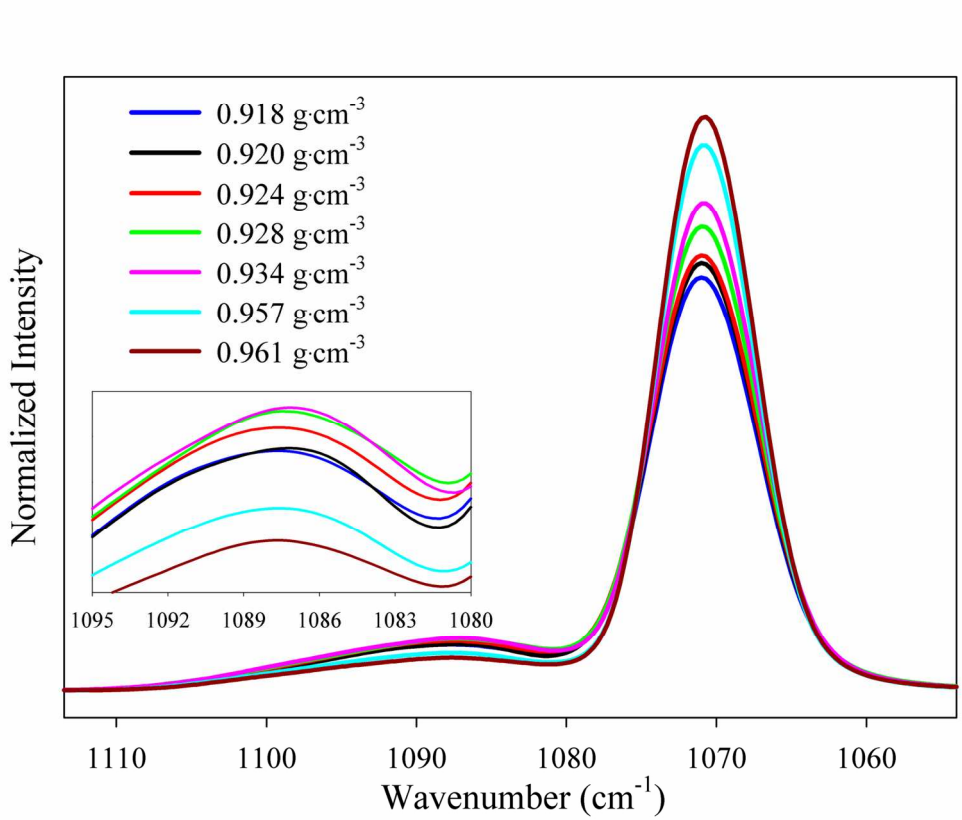

(a) Raman spectra of the low-density sample (0.918 g•cm-3) collected at -122 and 1.2 °C (the 1st and 15th snapshot, respectively) in the 1114-1054 cm-1 range, (b) Raman spectra of the low- (0.918 g•cm-3) and high-density (0.961 g•cm-3) PE pellets collected at -122 °C.
148x126mm (300 x 300 DPI)

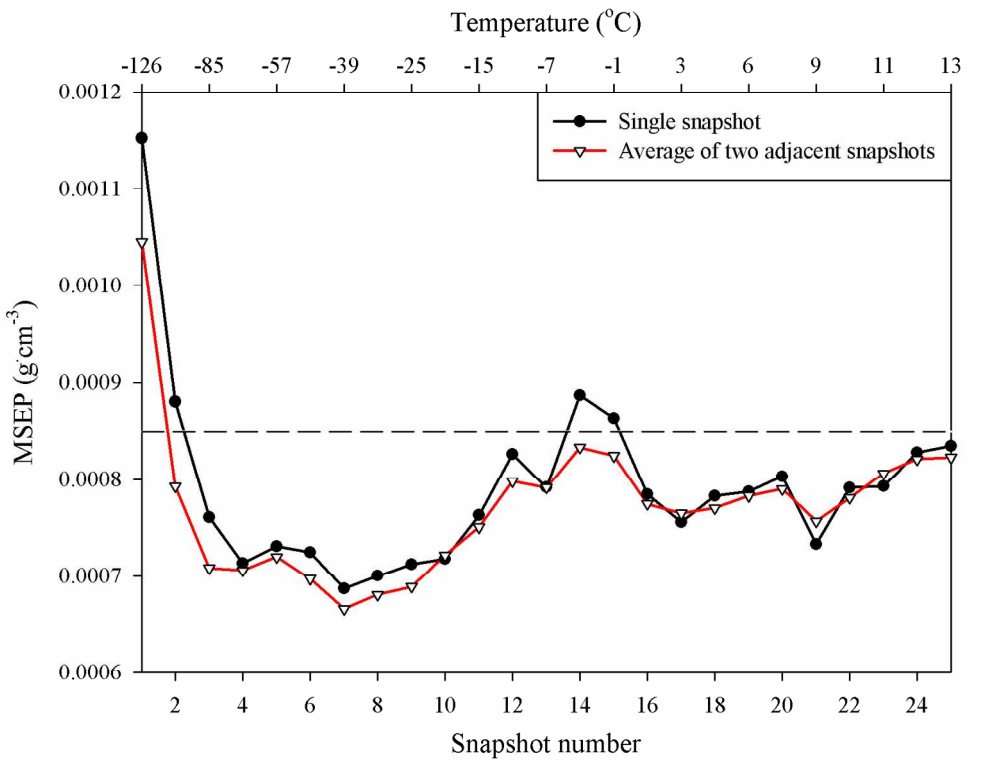

The MSEP obtained at each snapshot. Circles and triangles correspond to the results obtained from the use of a single snapshot and the average of two adjacent snapshots, respectively.
154x118mm (300 x 300 DPI)

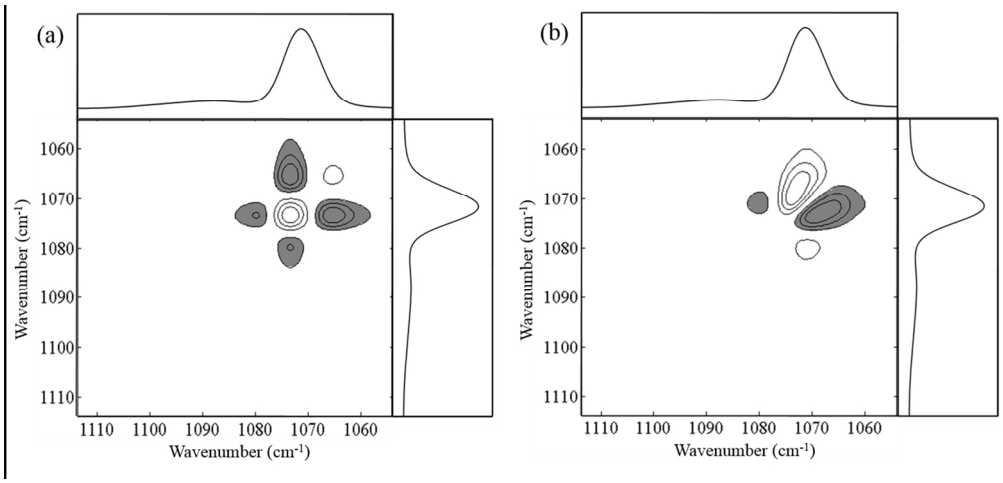

Synchronous (a) and asynchronous (b) correlation map calculated using all of the sample spectra collected in the 1st snapshot in the 1114-1054 cm-1 range.
259x122mm (150 x 150 DPI)

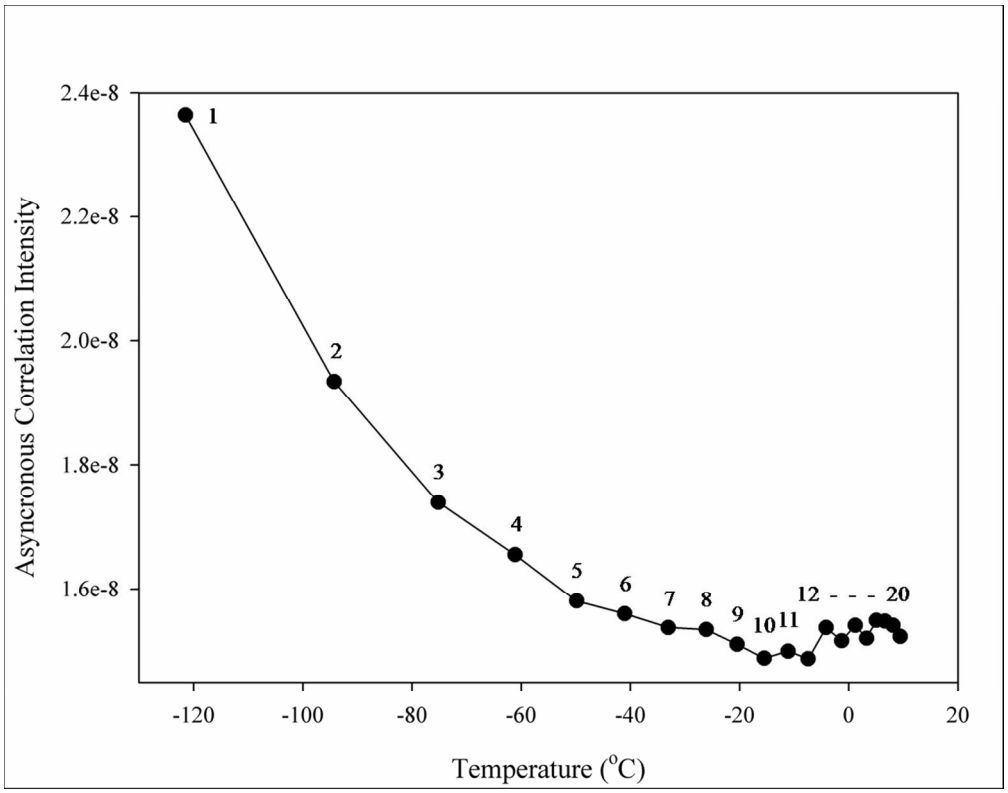

Variation in asynchronous correlation intensity between the crystalline and amorphous components as a function of measurement temperature. The numbers above each circle indicate the corresponding snapshot.
215x168mm (150 x 150 DPI)

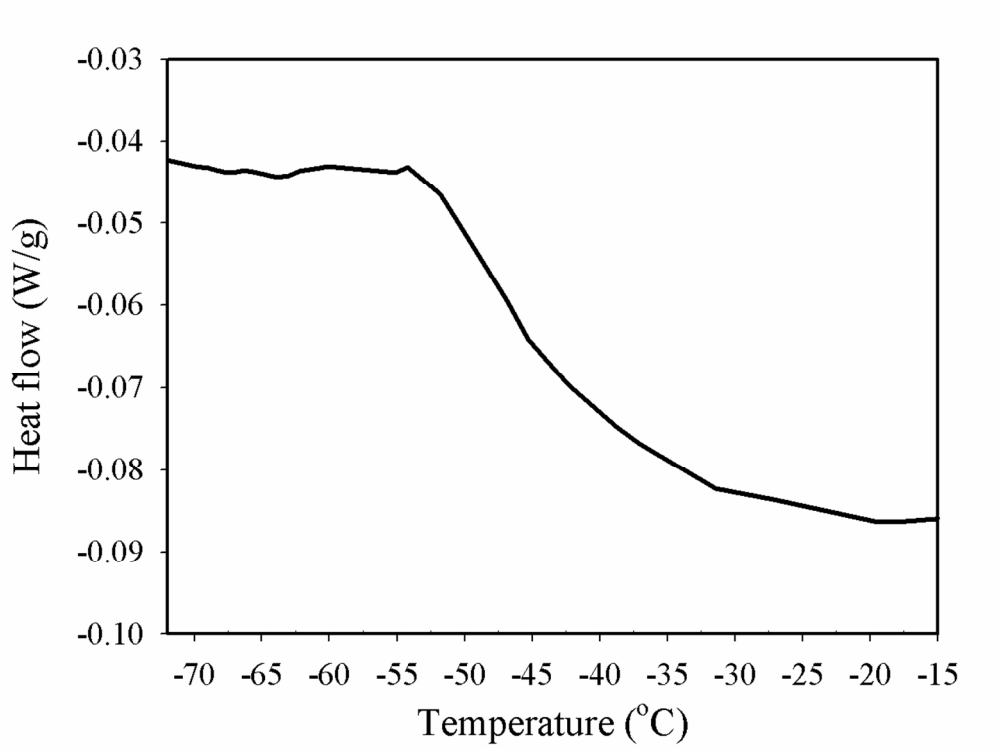

DSC curve of the low density (0.920 g·cm-3) in the temperature range from -72 to -15 oC.
109x82mm (300 x 300 DPI)

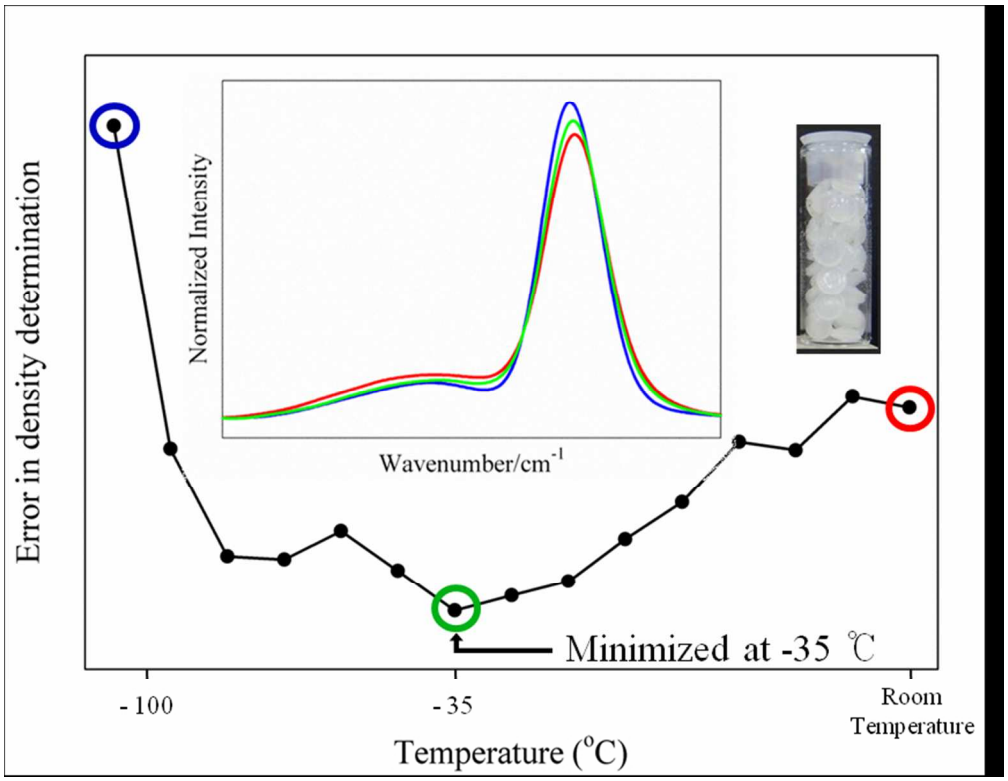

Graphical Abstract
146x112mm (150 x 150 DPI)

Measurement of polyethylene pellets near the glass transition temperature to enhance Raman spectral selectivity among samples and improve accuracy for density determination

Saetbyeol Kim,[a] Hideyuki Shinzawa,[b] Hoeil Chung[a]*and Yukihiro Ozaki[c]

[a]Department of Chemistry and Research Institute for Natural Sciences, Hanyang University, Seoul, Korea 133-791

[b]National Institute of Advanced Industrial Science and Technology (AIST), Nagoya, Japan 463-8560

[c]Department of Chemistry, School of Science & Technology, Kwansei-Gakuin University, Sanda, Hyogo, Japan 669-13

*Author to whom correspondence should be sent

Email: hoeil@hanyang.ac.kr

Tel.: 82-2-2220-0937

Fax: 82-2-2299-0762

Abstract

A simple and effective strategy for improving the accuracy for multivariate determination of polyethylene (PE) density using Raman spectroscopy has been demonstrated. This strategy is based on the possibility that varied polymeric structures of PE samples especially at a sub-zero temperature range would enhance their spectral selectivity, thereby potentially improving the multivariate correlation with their pre-determined physical properties such as density. For the evaluation, Raman spectra were collected with a regular interval during the continuous increase of PE temperature from cryogenic to near room temperature. Then, using partial least squares (PLS) regression, calibration models were developed to correlate Raman spectral features collected at each period with the reference PE density values. Interestingly, the accuracy was improved when the temperature of the PE pellets was -35 ^{o}C, near the glass transition temperature (T_g). To explain the improved accuracy, a two-dimensional (2D) correlation analysis was employed to detail the spectral variation induced by temperature change. Diverse segmental chain motions (so called micro-Brownian motion) predominantly occurring in the amorphous section of PEs around T_g majorly enhanced the spectral selectivity among PE samples. In addition, minor β-relaxation occurring around this temperature was an additional source for the enhanced spectral selectivity. In parallel, differential scanning calorimetry (DSC) curves of the samples were also examined to check the existence of the phase transitions.

Introduction

Previously, we searched an optimal temperature of 70 °C providing improved accuracy for Raman spectroscopic determination of the density of polyethylene (PE) pellets.[1] The origin for the improved accuracy was the enhanced spectral selectivity among the samples due to their diverse structural variations in the pre-melt stage at the found temperature and Raman spectroscopy was eventually effective to recognize phase transitions of polymer such as the pre-melting. The demonstrated strategy was simple since the spectral selectivity could be elevated by just maintaining sample temperature at a condition that could induce transient variation of polymeric structure.

When temperature of a polymer alternatively changes from sub-zero to cryogenic range, different types of phase transitions such as the glass transition could occur[2-3] and also enhance structural selectivity among samples possibly.[4] The nature of the glass transition and the existence of the dynamic divergence near glass transition temperature (T_g) have been studied by several research groups.[5-6] For examples, Xu *et al*. explored the nature of dynamics in the glass transition with the use of Dyre shoving model to explain the temperature dependence of polymer viscosity.[7] Wu *et al*. studied the dynamic response of the glass forming systems based on dynamic mechanical measurements.[8] The major challenge in these researches was to overcome the difficulty in obtaining reliable dynamic properties of a sample near and below T_g due to extremely long equilibrium relaxation time at these conditions. Owing to this fact, the essence of glass transition has not been fully understood yet. Therefore, studies of diverse analytical methods able to provide further insight on the glass transition are beneficial.

In this publication, we have examined Raman spectral variations of PE pellets in sub-zero to cryogenic temperature range to study possible phase changes such as the glass transition

and simultaneously searched conditions that could also enhance spectral selectivity among the samples to improve accuracy of their density determination using multivariate analysis. Spectral variations occurring in sub-zero to cryogenic temperature range are also expected to be different from sample to sample depending on the individual polymeric structures; therefore, a certain state leading to enhanced spectral selectivity among the samples would exist analogously. For this purpose, the PE pellets were rapidly cooled to a cryogenic temperature by simply placing a glass vial containing the samples in liquid nitrogen. Then, Raman spectra of the samples were collected at a regular interval while the sample temperature was increased naturally to near ambient temperature. By this way, Raman spectra of PE pellets over a wide temperature range could be easily collected without the use of any extensive peripheral devices.

The changes in PE band intensity, position and width as a function of temperature were initially examined in detail. Then, partial least squares (PLS) regression[9-10] was used to determine the density of PE pellets using the spectra collected at each period, and then the resulting accuracies were compared to identify an temperature range providing improved accuracy. It is necessary to clarify to avoid confusion that this study intends not to measure actual densities of PEs at sub-zero temperatures but to probe a Raman measurement temperature enabling of enhancing spectral discriminability among the samples to improve multivariate correlation with their density values pre-determined by using a standard ASTM method (density measurement at 23 ^{o}C).

Two-dimensional (2D) correlation analysis was used to assess Raman spectral variation of the samples according to the change in reference density as well as in temperature.[11-13] 2D correlation analysis is an effective method for investigating structural variation when external perturbations are applied to samples, as generally known. Finally, the results of 2D correlation analysis were directed to justify the improved accuracy of Raman measurement

performed within the selected temperature range.

Experimental Section

Samples, differential scanning calorimetry (DSC) analysis and Raman spectral collection

The 25 PE pellets adopted in a previous publication were also used in this study.[1,14] The samples were composed of three different grades (homo PE, 1-butene copolymerized PE and 1-octene copolymerized PE) with a density range of 0.918 - 0.961 g•cm^{-3}. Reference density of each sample was determined using a standard method described in ASTM D1505-3.[15] The PE pellets were simply transferred into a circular glass vial (diameter: 9.8 mm) for Raman spectral collection, as shown in Figure 1.

DSC curves of the samples were obtained over a temperature range from -179 to 15 ^{o}C using a TA Instruments model DSC2910 system (New Castle, DE, USA). Approximately 6.5 mg of sample taken from each pellet was transferred into a standard DSC aluminum pan for the analysis. The initial temperature was set to -179 ^{o}C for the cooling of a sample over 15 minutes and the sample was heated at a rate of 30 ^{o}C per minute until a final temperature reached to 15 ^{o}C. An empty pan was used for the reference.

Raman spectra were collected using the wide illumination (WAI) scheme (PhAT system, Kaiser Optical Inc., Ann Arbor, MI, USA), as previously described.[1,14] It was capable of illuminating a laser (785 nm) onto a large sample area with a diameter of 6 mm (area: 28.3 mm^2). The vial containing the PE pellets was initially immersed in liquid nitrogen to drive the sample temperature to a cryogenic level. After temperature equilibration for 15 minutes, the vial was taken out quickly and immediately positioned at the focal point of the WAI scheme for spectral collection. While the temperature of the samples was naturally increasing to near ambient temperature, Raman spectra were continuously collected at an interval of 20

seconds (laser exposure time: 20 seconds) and a total of 25 spectra (or snapshots) were collected for each sample.

The temperature of the samples was checked by inserting a thermocouple into the pellet packing. Triplicate spectra were collected for each sample. The same PE pellets were divided into three different vials, and then corresponding Raman spectra were separately collected as described above. The resolution of the collected spectra was 4 cm^{-1}. All spectral pre-processing and multivariate methods, including baseline correction, normalization, PLS and 2D correlation analysis, were performed using Matlab version 7.0 (Math Works Inc., MA, USA).

Results and Discussion

Raman spectral variations of PE pellets at different temperatures

Figure 1 shows pictures of low density PE pellets (density: 0.918 $g{\cdot}cm^{-3}$) in a glass vial during temperature elevation from cryogenic to near room temperature. The time at which the picture was taken is designated on each picture. As soon as the sample vial was taken out of the liquid nitrogen, frost immediately started to form on the wall and became thicker. The relative humidity in the lab was maintained at approximately 21.0 %. The frost was thickest at 2 minutes (corresponding to the 6^{th} spectral collection (hereinafter, snapshot), temperature around -45 ^{o}C) and became thinner thereafter. At 5 minutes (the 15^{th} snapshot, temperature around 1 ^{o}C), it started to disappear. Fortunately, frost (basically water) is a very weak Raman-scatterer, and so its influence on the overall spectral features of the PE pellets would not be substantial. In addition, the increase of pellet volume by approximately 9 % was observed during the temperature elevation due to the thermal expansion.

The temperature variation of the PE pellets is shown in Figure 2, where the *x*-axis is designated by both time and snapshot number. The curve in the figure corresponds to the

average of five independent temperature measurements from five separate batches prepared from the same PE pellets. Bars on each snapshot indicate the corresponding standard deviations of temperature measurements. The rate of temperature elevation is faster at the earlier stages and substantially slower at the later stages. Therefore, the magnitude of the error bar is relatively larger in the earlier stages.

Figure 3 (a) shows Raman spectra (1504-1054 cm^{-1} range) of the low density PE sample (density: 0.918 $g{\cdot}cm^{-3}$) collected at different snapshots (temperatures). Although a total of 25 Raman spectra was collected during the elevation of temperature, only 5 Raman spectra were selected for easier comparison of spectral features. In addition, a Raman spectrum obtained at room temperature (23 ^{o}C) is also shown. PE Raman bands are clearly observable in each snapshot, while the baselines of the spectra vary minutely due to the presence of frost on the wall of the vial.

To compare the spectral features in each snapshot, the spectra were normalized. The baseline-corrected spectrum at five different wavenumbers (1504, 1402, 1196, 1114 and 1054 cm^{-1}) was divided by the corresponding peak area under the 1504-1054 cm^{-1} range for the normalization. Four narrower spectral ranges of 1490-1405, 1310-1290, 1190-1120 and 1100-1055 cm^{-1} are highlighted in Fig. 3 (b), (c), (d) and (e), respectively. For easier tracking of the spectral variation, the changes in the maximum peak positions and the corresponding intensities of the major bands are also shown in the insets. The magnitudes of *x*- and *y*-span of the inset plots are same. In the 1490-1405 cm^{-1} range (Fig. 3 (b)), where the 1464 (CH_2 rocking), 1443 (CH_2 bending) and 1420 cm^{-1} (CH_2 bending) bands at room temperature are present,[1,14,16-21] the shape of the bands clearly varies as the temperature increases. The 1464 cm^{-1} band shifts to 1469 cm^{-1} at -126 ^{o}C (1st snapshot). Then, it moves to a lower wavenumber, and its bandwidth broadens in the following snapshots. Conversely, the 1420 cm^{-1} band shifts to 1416 cm^{-1} at -126 ^{o}C. Then, it moves to higher wavenumbers and its

bandwidth marginally broadens with temperature elevation. The 1443 cm^{-1} band shifts to a slightly higher wavenumber at -126 ^{o}C, while the corresponding intensity decreases and the bandwidth becomes broader as the sample temperature increases.

The 1298 cm^{-1} (CH_2 twisting) band at room temperature shifts slightly to 1297 cm^{-1} at -126 ^{o}C (1st snapshot), as shown in Fig. 3 (c). Then, it moves to higher wavenumbers with increasing temperature. In Fig. 3 (d), the 1177 (CH_2 rocking) and 1138 cm^{-1} (C-C stretching) bands show similar behavior upon temperature perturbation as does the 1464 cm^{-1} band. In Fig. 3 (e)), the 1070 cm^{-1} band (C-C anti-symmetric stretching) corresponding to the crystalline component in PE and the broad spectral features around 1085 and 1065 cm^{-1} originated from the amorphous structure[16-21] are shown. With an increase in the sample temperature, the intensity of the crystalline peak decreases and the intensity of the amorphous peak synchronously increases. This indicates that the structure becomes more crystalline at very low temperature.

The superior repeatability of measurement is necessary to recognize minute spectral variation induced by temperature change. To assess the repeatability, standard deviations (SDs) of intensities at each wavenumber were calculated using independently collected triplicate spectra in each case. Fig. 3 (f) presents SDs of intensities calculated from the spectra shown in Fig. 3 (e). It is important to note that the *y*-span is 100 times smaller compared that in Fig. 3 (e). The magnitudes of SDs are very small and the average SD of these observations is 3.3×10^{-6} normalized absorbance unit (AU). In the meanwhile, the magnitude of intensity change of the 1070 cm^{-1} peak between the measurements at -126 (1st snapshot) and 8 ^{o}C (20th snapshot) is 0.000263 normalized AU, so the average intensity change between the adjacent snapshots is 1.38×10^{-5}. The magnitude of average SD relative

to that of average intensity change per snapshot is 24 %, so the measurement is sufficiently precise to perceive the temperature-induced spectral variation between the snapshots.

All of the spectral variations described above were more significant at the lower temperature (earlier snapshots) and most of the PE bands broadened with temperature elevation. The same spectral variations shown in Fig. 3 were also examined for the middle (0.934 $g \cdot cm^{-3}$) and high (0.961 $g \cdot cm^{-3}$) density samples, although the corresponding figures are not shown here. The trends in spectral variations for these samples were similar to that observed for the low density PE in Fig. 3, while the magnitude of spectral variation and the change in band shape upon temperature perturbation were slightly different.

Figure 4 shows Raman spectra of seven selected PE samples of low to high densities measured at -126 °C (the 1st snapshot). The inset highlights the spectral variations in the 1095-1080 cm^{-1} range. The intensities of the 1070 cm^{-1} band were higher for the high density PEs than the low density PEs. This obviously indicates a larger fraction of crystalline component in the high density PEs. By contrast, the intensities of the amorphous bands were relatively higher for the low density PEs. Examination of the spectra in Fig. 3 (e) and Fig. 4 confirms that the intensities of crystalline and amorphous bands of PE pellets vary with both temperature and density. Therefore, the temperature-induced spectral variations of PE samples are expected to be highly diverse each other. Thus, the accuracy of measurement at each snapshot could be dissimilar due to the altered spectral features of the samples by temperature change.

Determination of the density of PE pellets in each snapshot

Partial least squares (PLS) method[9,10] was used to determine the density of the PE pellets using Raman spectra collected at each snapshot. Initially, 20 and 5 samples were assigned to

the calibration and validation sets, respectively. All combinations of the selected five samples as the validation set were tested, and the mean standard error of calibration (MSEC) and the mean standard error of prediction (MSEP) were calculated by averaging the individual SEC and SEP values for each combination as performed in a previous study.[8,14] The 1504-1054 cm^{-1} range shown in Fig. 3 (a) was used for PLS.

The MSEPs obtained at each snapshot (circles) are displayed in Figure 5. The corresponding measurement temperatures are also indicated on the upper *x*-axis. In all cases, six PLS factors were used. The dashed line indicates the MSEP acquired from the measurement at room temperature (designated as $MSEP_{RT}$), which was 0.00084 $g{\cdot}cm^{-3}$, comparable to the MSEP (0.00080 $g{\cdot}cm^{-3}$) achieved in a previous study.[14] From the 1st to 4th snapshots (sample temperature from -126 to -69 °C), the MSEP dropped sharply below the $MSEP_{RT}$ and then reached a minimum at the 7th snapshot (-39 °C), an MSEP of 0.00068 $g{\cdot}cm^{-3}$. After the 7th snapshot, it gradually increased again. In comparison with the $MSEP_{RT}$, the improved accuracy at the 7th snapshot was statistically significant based on a *t*-test at a 95% confidence level.

Since the increase of temperature was much faster and the uncertainty in sample temperature was larger in the lower temperature range, a doubled laser exposure time of 40 seconds for spectral acquisition could somewhat lessen the temperature uncertainty. Therefore, spectra acquired in two adjacent snapshots were continuously averaged, and these averaged spectra were used for PLS. For example, the 1st and 2nd snapshots were averaged to yield a new 1st snapshot, and the 2nd and 3rd snapshots were averaged to generate a new 2nd snapshot. Each averaged spectrum was equivalent to spectral collection over 40 seconds of laser exposure. The MSEP obtained for each averaged snapshot (triangles) is also shown in the figure. Six factors were also used for each case. The variation in MSEPs obtained using

two-snapshot averaged spectra was similar to that using single-snapshot spectra, while the MSEPs were slightly lower. The lowest MSEP (0.00066 $g \cdot cm^{-3}$) was achieved at the 7th snapshot, corresponding to the average of the original 7th and 8th snapshots. When the snapshots were further averaged, i.e., by averaging three adjacent snapshots, there was no additional improvement in MSEP. The overall results indicate that PLS accuracy for the determination of PE density is improved by spectral acquisition around -35 ^{o}C. This finding implies that the spectral features of PE pellets around -35 ^{o}C are more descriptive to follow the variation in densities determined using the ASTM method.[22-23]

2D correlation analysis

Justification for the improved accuracy around -35 ^{o}C needs to provide. Since the temperature-induced spectral variations of the PE samples are rather complicated, two dimensional (2D) correlation analysis could be effective for examining the complexly different structural variations of the PEs induced by temperature. A detailed description of 2D correlation analysis can be found in other publications.[11-13] The 1115-1054 cm^{-1} range containing both crystalline and amorphous bands was used for the analysis.

Figure 6 (a) shows the synchronous map generated using all the sample spectra of varying densities collected at -126 ^{o}C (1st snapshot). The auto-correlation peak around 1073 cm^{-1}, indicating the gradual increase in the crystalline with the increase of sample density, is clearly shown. The development of negative cross-correlation peaks (shaded) between 1070 and 1060 cm^{-1} implies that the change in the intensity of these two bands occurred in the opposite direction, confirming the simultaneous increase and decrease of the crystalline and amorphous components, respectively.

Fig. 6 (b) shows the apparent asynchronous correlation peak between 1073 and 1060 cm^{-1}. This informs that structural variation in the amorphous component occurred prior to

that in the crystalline component. Such a sequential structural change suggests that the intensity variation in the crystalline and amorphous components is not complementary, in other words, no see-saw type variation occurs between these two components. Thus, the structural variations of the samples at -126 ^{o}C are nonlinear. This nonlinear behavior is probably due to the occurrence of a new component possessing a partially ordered structure. Therefore, a decrease in the amorphous structure is not linearly compensated for by an increase in the crystalline structure due to the presence of this intermediate structure. This result is consistent with the previous report by Noda et al. that PE polymers undergoing transient melting showed a specific phase transition from crystalline lamellae to amorphous via the development of a partially deformed structure.[13,24] The partially deformed structure could provide additionally valuable information to possibly enhance spectral discrimination among PE samples and improve multivariate correlation with a target sample property.

The asynchronous correlation informs the occurrence of new partially ordered structures; while, its intensity becomes lower when the more of these structures present. So, the examination of asynchronous correlation intensity is beneficial to probe the temperature-induced spectral variations as shown in Figure 7. The asynchronous correlation intensity in the 1073-1060 cm^{-1} range was calculated and the numbers above each circle indicate the corresponding snapshots. The intensity gradually decreased as the sample temperature increased and its variation was rather minor after -39 ^{o}C. This implies that the diverse spectral variations occurring in the amorphous and partially ordered regions become more significant around this temperature. At an ultra-low temperature, the amorphous structure in PE is in a glassy state, where molecules are only able to vibrate marginally without distinct segmental motion. When the temperature of a sample increases further and reaches its glass transition temperature (T_g), molecules start to wiggle and these diverse wiggling motions (so-called micro-Brownian motion) transform a sample to a rubbery state. As is generally known,

the second T_g of PE is approximately around -40 ^oC,[25-27] close to the temperature providing the improved accuracy. The degree of micro-Brownian motion could differ depending on the amount of amorphous component in a sample, and also its behavior could vary from sample to sample. Thus, this is a major source for enhancing the spectral discriminability among PE samples. In addition, previous publications showed the phase change of PEs associated with β-relaxation occurring around -35 ^oC,[28-30] while the resulting structural change was very small. This relaxation is originated from initiation of molecular motion of short chain branches in the interfacial regions (between crystalline and amorphous components) of the lamellae. Therefore, it also partially contributes to the enhancement of spectral selectivity.

To alternatively confirm the structural variation around -40 ^oC, DSC curves of all 25 PE samples measured and examined. Figure 8 shows DSC curve of the low density PE sample (0.920 $g \cdot cm^{-3}$) in the temperature range from -72 to -15 ^oC. The decrease of heat flow in the curve around -40 ^oC is clearly apparent and so it suggests the onset of the glass transition. In the meanwhile, no meaningful changes were observed in the DSC curves of the other samples. The absence of transition peaks for these samples is acceptable because the behaviors of coexisting amorphous and crystalline structures in a sample at glass transition are in thermally opposite direction. Glass transition can be seen as the relaxation of branches in a polymer chain that occurring mainly in disordered amorphous structure, while the progress of relaxation is also hindered by the development of polymer chain folding resulting in ordered lamellae structure. Since the relaxation of branches and the chain folding are opposite in the direction of heat flow, the net heat flow could be too minute to be observed in DSC curves. It is most probable that the above sample showed the apparent transition in Fig. 8 has relatively larger degree of structural relaxation in the amorphous structure compared to

the other samples. The mentioned both structural variations actually occur around -40 ^{o}C, although they are hardly detectable in the DSC curves.

The MSPE achieve here is slightly inferior compared to that (0.00059 g·cm^{-3}) in our previous publication in which the same samples were measured at 70 ^{o}C. The DSC peaks around 70 ^{o}C indicating the pre-melting behaviors were more apparent compared to those of the glass transition in this study. The larger degree of structural relaxation by pre-meting enhanced the spectral discriminability among the samples further and the better accuracy was thereby a consequence. Nonetheless, the enhanced spectral discriminability at the glass transition temperature also helps to improve the accuracy of the measurement compared to that of the room temperature measurement.

Conclusion

The acquisition of Raman spectra of PE pellets around their T_gs enhanced the spectral selectivity among the samples due to micro-Brownian motions occurring in the amorphous component and minor β-relaxation, and eventually improved multivariate correlation of the spectra with the corresponding sample property (density). 2D correlation analysis effectively described the spectral variations occurring in the amorphous and crystalline components, and provided further insight into the glass transition of PE which has not been fully understood. The analytical strategy described here is simple and expandable to measure properties of other polymeric samples since many polymers have phase transition states such as glass transitions, which could enhance spectral selectivity among samples.

For real application of the strategy, several issues need to further consider. Inclusion of more samples with diverse grades in a calibration dataset will be necessary for robust routine analysis. In addition, when samples with largely different shapes are measured, the possible

shape-dependent spectral variation that would degrade accuracy of measurement needs to examine. Since the WAI scheme is used for the acquisition of spectra and Raman peaks are normalized, no significant shape-dependent spectra are expected when appearances of samples are moderately dissimilar such as the PE samples in this study. As long as the above-mentioned issues are under control, the proposed method will be versatile for multivariate quantitative spectroscopic analysis of polymers.

Acknowledgements

This research was supported by Basic Science Research Program through the National Research Foundation of Korea (NRF) funded by the Ministry of Education, Science and Technology (NRF-2012R1A1B3003965)

Reference

1. S. Chan Park, H. Shinzawa, J. Qian, H. Chung, Y. Ozaki and M. A. Arnold, The Analyst, 2011, **136**, 3121-3129.
2. G. R. Strobl, The Physics of Polymers, Springer, Berlin Heidelberg, 2007.
3. E. –J. Donth Relaxation and Thermodynamics in Polymers: Glass transition, Akademie, Verlag, 1992.
4. C. A. Angell, K. L. Ngai, G. B. McKenna, P. F. McMillan, and S. W. Martin, J. Appl. Phys. 2000, **88**, 3113-3157.
5. K. L. Ngai, S. Capaccioli, M. Paluch, and D. Prevosto, J. Phys. Chem. B 2014, **118**, 5608-5614.
6. J. Zhao, S. L. Simon and G. B. McKenna, Nat. Commun. 2013, **4**, 1783.
7. B. Xu and G. B. McKenna. J. Chem. Phys. 2011, **134**, 124902.
8. J Wu, G Huang, X Wang, X He, B Xu, Macromolecules 2012, **45**, 8051-8057.
9. K. R. Beebe, R. J. Pell and M. B. Seasholtz, Chemometrics: A Practical Guide, John Wiley and Sons, New York, 1998.
10. K. R. Beebe, B. R. Kowalski, Anal. Chem., 1987, **59**, 1007A.
11. I. Noda, Appl. Spectrosc., 1993, **47**, 1329–1336.
12. I. Noda, Appl. Spectrosc., 2000, **54**, 994–999.
13. I. Noda and Y. Ozaki, Two-dimensional Correlation Spectroscopy, Willey and Sons, Chichester, West Sussex, 2004.
14. M. Kim, J. Noh and H. Chung, Analytica chimica acta, 2009, **632**, 122-127.
15. Method D1505-3, Annual Book of ASTM (American Society for Testing and Materials), Philadelphia, 2003.

16. H. Sato, M. Shimoyama, T. Kamiya, T. Amari, S. Šašić, T. Ninomiya, H. W. Siesler and Y. Ozaki, J. Appl. Polym. Sci., 2002, **86**, 443–448.

17. T. Furukawa, H. Sato, Y. Kita, K. Matsukawa, H. Yamaguchi, S. Ochiai, H. W. Siesler and Y. Ozaki, Polym. J., 2006, **38**, 1127–1136.

18. P. A. Bentley and P. J. J. Hendra, Spectrochim. Acta, Part A, 1995, **51**, 2125–2131.

19. A. Tarazona, E. Koglin, B. B. Coussens and R. J. J. Meier, Vib. Spectrosc., 1997, **14**, 159–170.

20. K. Sano, M. Shimoyama, M. Ohgane, H. Higashiyama, M. Watari, M. Tomo, T. Ninomiya, and Y. Ozaki, Appl. Spectrosc., 1999, **53**, 551-556

21. K Tashiro, S. Sasaki, M. Kobayashi, Macromolecules, 1996, **29**, 7460.

22. K. P. J. Williams and N. J. Everall, J. Raman Spectrosc., 1995, **26**, 427.

23. N. Everall, P. Tayler, J. M. Chalmers, D. McCarron, R. Forward and J. H. van deer Maas, Polymer, 1994, **35**, 3184.

24. I. Noda, G. M. Story and C. Marcott, Vib. Spectrosc., 1999, **19**, 461–465.

25. O. Alexiadis, V. G. Mavrantzas, R. Khare, J. Beckers, and A. R. C. Baljon, Macromolecules, 2008, **41**, 987-996

26. G. T. Davis and R. K. Eby, J. Appl. Phys., 1973, **44**, 4274-4281

27. C. Vasile, Handbook of Polyolefins, CRC press, London, 2000.

28. S. Fakirov and B. Krasteva, J. Macromol. Sci., Phys., 2000, **39**, 297–301.

29. P. J. Hendra and C. Passingham, Eur. Polym. J., 1991, **27**, 127-134.

30. N. Alberola, J. Y. Cavaille and J. Perez, Eur. Polvm. J., 1992, **28**, 935-948.

Figure Legends

Figure 1. Pictures of the low density PE pellets (density: 0.918 g·cm^{-3}) in a glass vial during the temperature elevation from cryogenic to near room temperature.

Figure 2. Temperature variation of PE pellets as a function of time, in which the *x*-axis is designated by both time and snapshot number. The curve corresponds to the average of five independent temperature measurements from five separate batches prepared from the same PE pellets. Bars in each snapshot indicate the corresponding standard deviations of temperature measurements.

Figure 3. (a) Raman spectra of the PE sample (density: 0.918 g·cm^{-3}) collected during different snapshots in the 1504-1054 cm^{-1} range. To examine the spectral features in detail, the corresponding normalized spectra were highlighted in four different narrower spectral ranges: (b) 1490-1405, (c) 1310-1290, (d) 1190-1120 and (e) 1110-1055 cm^{-1}. Standard deviations (SDs) of intensities in the 1110-1055 cm^{-1} range calculated using independently collected triplicate spectra are also shown (f).

Figure 4. (a) Raman spectra of the low-density sample (0.918 g·cm^{-3}) collected at -122 and 1.2 °C (the 1st and 15th snapshot, respectively) in the 1114-1054 cm^{-1} range, (b) Raman spectra of the low- (0.918 g·cm^{-3}) and high-density (0.961 g·cm^{-3}) PE pellets collected at -122 °C.

Figure 5. The MSEP obtained at each snapshot. Circles and triangles correspond to the results obtained from the use of a single snapshot and the average of two adjacent snapshots, respectively.

Figure 6. Synchronous (a) and asynchronous (b) correlation map calculated using all of the sample spectra collected in the 1st snapshot in the 1114-1054 cm^{-1} range.

Figure 7. Variation in asynchronous correlation intensity between the crystalline and amorphous components as a function of measurement temperature. The numbers above each circle indicate the corresponding snapshot.

Figure 8. DSC curve of the low density (0.920 g·cm^{-3}) in the temperature range from -72 to -15 ^{o}C.